A PRACTICAL EVALUATION OF ROBUST CONTROLLERS DESIGNED WITH VARIANTS OF THE LQG/LTR METHOD

Karl Heinz Kienitz, kienitz@ieee.org
Renan Lima Pereira, renanlimaster@gmail.com
Instituto Tecnológico de Aeronáutica, Divisão de Engenharia Eletrônica
São José dos Campos - SP, 12228-900, Brazil

Abstract. *In this paper we investigate the design of robust fixed parameter controllers, designed using the TFL/LTR (Target Feedback Loop/Loop Transfer Recovery) technique using two controller structures that will be evaluated with sets of specifications for the robust stability and performance of a laboratory helicopter model with three degrees of freedom. This helicopter is an underactuated nonlinear system, having three degrees of freedom and two actuators. The laboratory model was produced by Quanser Consulting and simulates typical behaviors of an aircraft in a helicopter "tilt-motor" configuration with rigid body motion. It allows the evaluation of various techniques for multivariable control. The dynamics of the helicopter can be described by a 6th order model taking as state variables the angles of travel ϕ, elevation ψ and pitch θ and associated rates. The first structure considered in the evaluation is, the LQG/LTR compensator, used as a reference for performance evaluation. The second structure is a variation of the LQG/LTR method, which uses the "Gain-Scaled Kalman Filter" (GSKF) to obtain desired dynamics and the "Amplified Linear Quadratic Regulator" (ALQR) for loop recovery as well as consequent determination of the compensator which guarantees the attainment of dynamics as close as possible to the desired dynamics. For both techniques, designed compensators shall solve the problem of stable tracking of reference trajectories, ensuring performance and robust stability, in spite of disturbances, noise and unmodeled dynamics, including unstructured modeling errors in high frequencies. Finally, we present experimental results obtained with the application of the two robust compensators for tracking problems of the helicopter with three degrees of freedom.*

Keywords: *Robust Control, TFL/LTR controllers, 3DOF Helicopter*

1. INTRODUCTION

Robust controller design has received much attention in control systems research. There are several techniques of robust control system design available in the literature (Skogestad and Postlethwaite, 2001), (da Cruz, 1996). One potential approach, termed Target Feedback Loop/Loop Transfer Recovery (TFL/LTR) has emerged successfully in recent years and application to a wide class of situations. It stands for a general class of robust controller design procedures which are carried out in two sequential steps, namely, TFL-design and LTR.

Two different compensator structures are considered in this paper for TFL/LTR technique. One is a traditional LQG/LTR structure (Linear Quadratic Gaussian/Loop Transfer Recovery) which is used in the more recent gain scheduling methodology approach. Lacking specific name, the other structure will be designated as structure #2, this structure is presented in (Prakash, 1990). It consists of the combination of Gain-Scaled Kalman Filter (GSKF) and Amplified Linear Quadratic Regulator (ALQR) to recover a system with favorable guaranteed stability margins.

This paper is organized as follow. Section 2 contains the system description. Section 3 presents the robust control methodology. Section 4 describes problem formulation and its design control specifications are chosen for robust stability and performance. Section 5 describes the design of TFL/LTR controllers . Section 6 shows the results and discussions. Finally, section 7 contains the conclusion.

2. DESCRIPTION OF THE 3DOF HELICOPTER

The system considered in this paper is a practical evaluation model of the Quanser three-degree-of-freedom helicopter (Figure 1). The system is composed by the helicopter body, which is a small arm with one propeller at each end, and the helicopter arm, which connects the body to a fixed base. Although the system cannot exhibit translational motion, as it is fixed in a support, it can rotate freely about three axes. The helicopter position is characterized by the pitch, travel and elevation angles. The pitch movement corresponds to the rotation of the helicopter body about the helicopter arm, the travel movement corresponds to the rotation of the helicopter arm about the vertical axis and the elevation movement corresponds to the rotation of the helicopter arm about the horizontal axis.

Figure 1. 3DOF helicopter

The control variables are the input voltages to the power amplifiers that drive each one of the two DC motors connected to the helicopter propellers. The maximum input voltage to the amplifiers is 5 V. Three digital encoders provide measurements of the helicopter angles. Encoder resolution is about 0.044 degree for travel angle and 0.088 degree for pitch and elevation angles.

A nonlinear sixth-order model for the helicopter, which does not include the quantization effect due to the encoders, was derived in (Lopes, 2007) and refined in (Maia, 2008). The model has the form shown in Eq. (1), where x_1 is the pitch angle (in rad), x_2 is the pitch rate (in rad/s), x_3 is the elevation angle (in rad), x_4 is the elevation rate (in rad/s), x_5 is the travel angle (in rad), x_6 is the travel rate (in rad/s), u_1 is the front motor amplifier input voltage (in V), u_2 is the back motor amplifier input voltage (in V), and the remaining symbols represent constants determined experimentally.

$$
\begin{aligned}
&\dot{x}_1 = x_2 \\
&\dot{x}_2 = \xi_{16}\left\{\xi_1(u_1^2 - u_2^2) + \xi_2(u_1 - u_2) - \nu_2 x_2\right\} \\
&\dot{x}_3 = x_4 \\
&\dot{x}_4 = x_6^2\left\{\xi_3 sin2x_3 + \xi_4\cos 2x_3\right\} + \xi_5 sinx_3 + \xi_6\cos x_3 + \left\{\xi_7(u_1^2 + u_2^2) + \xi_8(u_1 + u_2)\right\}\cos x_1 \\
&\dot{x}_5 = x_6 \\
&\dot{x}_6 = \left\{\xi_{13} + \xi_{14}\sin 2x_3 + \xi_{15}\cos 2x_3\right\}^{-1}\left\{\nu_1 - \nu_3 x_6 + \left[\xi_9\left(u_1^2 + u_2^2\right) + \xi_{10}\left(u_1 + u_2\right)\sin(x_1)\right] + \right. \\
&\left. x_4 x_6\left[\xi_{11}\sin 2x_3 + \xi_{12}\cos 2x_3\right]\right\}
\end{aligned}
\tag{1}
$$

2.1 Linearized Model

The robust control formulations adopted require a linearized model representing the system dynamics. The model to be used in the design of the controllers was obtained by linearization around an equilibrium point. Taking the parameters $\xi_{1,\ldots,}\xi_{16}$, ν_2 and ν_3 as in (Maia, 2008), and choosing ν_1 = 0, for simplicity, so that the balance occurs at the helicopter horizontally, we have the following matrices for the linearized model helicopter around this equilibrium point (x_{eq} = 0; u_{1eq} = u_{2eq} = 2.9735V). (Rubens, 2009)

$$
A = \begin{bmatrix}
0 & 1 & 0 & 0 & 0 & 0 \\
0 & -0.7530 & 0 & 0 & 0 & 0 \\
0 & 0 & 0 & 1 & 0 & 0 \\
0 & 0 & -1.0389 & 0 & 0 & 0 \\
0 & 0 & 0 & 0 & 0 & 1 \\
-1.3426 & 0 & 0 & 0 & 0 & -0.4377
\end{bmatrix}, \quad
B = \begin{bmatrix}
0 & 0 \\
2.966 & -2.966 \\
0 & 0 \\
0.4165 & 0.4165 \\
0 & 0 \\
0 & 0
\end{bmatrix}
\tag{2}
$$

3. CONTROL DESIGN METHODOLOGY: TFL/LTR TECHNIQUES

The TFL/LTR approach of designing robust controllers falls under a broader category of procedures in which the robustness is ensured by certain loop properties. It consists of two sequential steps, namely, TFL design, characterized by calculating of the constant TFL-gain matrix, K_f, that specifies stability and robustness performance and the LTR step, in the determination of the constant LTR gain matrix, K_r, to recover the loop transfer.

The TFL/LTR controllers are fixed controllers. In other words, the parameters of the TFL/LTR controllers are calculated in the design process and remain fixed throughout system operation. However, the structure of the TFL/LTR controllers is not a unique one. Two different structures will be considered in this paper.

3.1 Structure I - (LQG/LTR)

Block diagram representation of the controller structure $\#1$ is shown in Figure 2. The equations representing the compensator are

$$\begin{aligned} \dot{z}(t) &= Az(t) + Bu(t) + K_f\left[-e(t) - Cz(t)\right], \\ u(t) &= -K_r z(t) \end{aligned} \tag{3}$$

We choose to represent the controllers by the triplet $\{A_k, B_k, C_k\}$.With, structure $\#1$, the coefficient matrices of the triplet will be

$$A_k = (A + K_f C + BK_r);\;\; B_k = -K_f;\;\; C_k = -K_r \tag{4}$$

The transfer function of the $m \times m$ controller is given by

$$K(s) = K_r(sI - A + K_f C + BK_r)^{-1}K_f \tag{5}$$

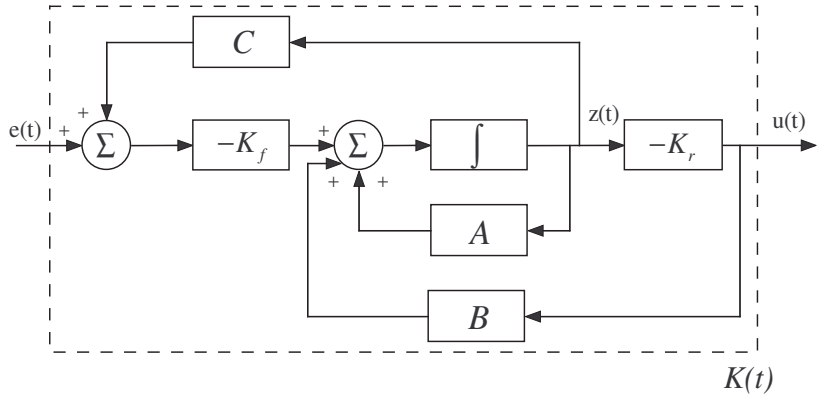

Figure 2. Block schematic of structure $\#1$

For the structure $\#1$, we use the technique TFL/LTR described in (Athans, 1986). In this procedure the TFL-gain, K_f, is calculated using the standard Kalman filter, that will meet the stability and robust performance. In step LTR is determined the LTR-gain, K_r, characterized by the linear regulator quadratic (LQR) that recovers the desired loop transfer function. For detailed presentations of the method refers to (Athans, 1986) and (da Cruz, 1996).

3.2 Structure II

Block diagram representation of the controller structure $\#2$ is shown in Figure 3. The equations representing the compensator are

$$\begin{aligned} \dot{z}(t) &= Az(t) + Bu(t) - K_f e(t), \\ u(t) &= -K_r z(t). \end{aligned} \tag{6}$$

where $z(t)$ is the compensator state vector, *A*, *B* and *C* are coefficient matrices of the design model, and K_f and K_r are the gain matrices. Using Eq. (7), the dynamic equation can be rewritten as

$$\dot{z}(t) = (A - BK_r)z(t) - K_f e(t) \tag{7}$$

We choose to represent the controllers by the triplet $\{A_k, B_k, C_k\}$. With, structure $\#2$, the coefficient matrices of the triplet will be

$$A_k = (A - BK_r);\;\; B_k = -K_f;\;\; C_k = -K_r \tag{8}$$

The transfer function of the controller for structure $\#2$ from $e(s)$ to $u(s)$ is given by

$$K(s) = K_r(sI - A + BK_r)^{-1}K_f \tag{9}$$

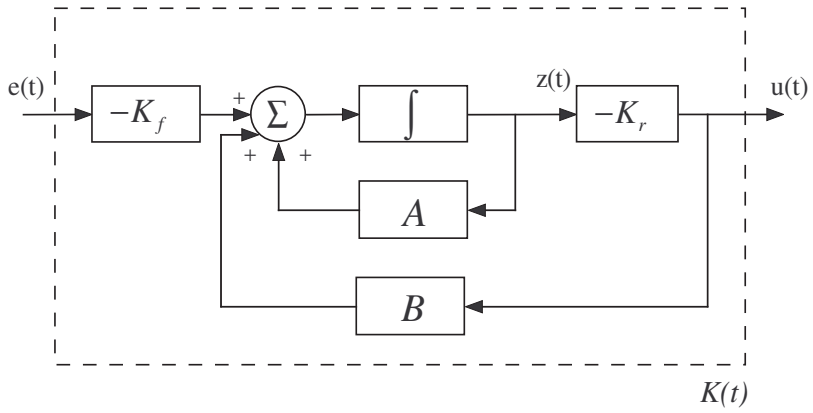

Figure 3. Block schematic of structure $\#2$

The difference between structure $\#2$ and the conventional structure $\#1$ is that the $-K_f Cz(t)$ term is absent in Eq. (7) as compared with Eq. (3). A comparison of Figure 2 and Figure 3 will reveal which link of structure $\#1$ is opened to get structure $\#2$. Experience shows that this modification quickens the loop transfer recovery process.

3.2.1 Gain Scaled Kalman Filter (option for the TFL step)

The GSKF will be introduced as a state estimator, in concordance with the description of the KF given in (Athans, 1986), (C.Doyle and Stein, 1981). Consider a system described by:

$$\begin{aligned} \dot{x}(t) &= Ax(t) + Bu(t) + E\xi(t), \\ y(t) &= Cx(t) + n(t), \end{aligned} \tag{10}$$

where, $\xi(t)$ and $n(t)$ are vector random processes called process noise (disturbance) and measurement noise, respectively. The system may be considered as the design model together with the disturbance and noise. The design model *A, B, C* is assumed to be detectable, and *C* is assumed to be of full rank. The GSKF has the form

$$\dot{\hat{x}}(t) = A\hat{x}(t) + Bu(t) + K_f\left[y(t) - C\hat{x}(t)\right] \tag{11}$$

The filter gain matrix is given by

$$K_f = (1/\beta)PC^T R^{-1} \tag{12}$$

where $0 < \beta < 1$ and $P = P^T \geq 0$ is the solution of the filter algebraic Riccati equation (FARE)

$$AP + PA^T + Q - PC^T R^{-1} CP = 0 \tag{13}$$

with some $Q = Q^T \geq 0$ and $R = R^T > 0$. Clearly, the GSKF-gain is the KF-gain scaled by $1/\beta$. The error dynamics of estimator GSKF is defined as

$$\dot{e}(t) = (A - K_f C)\, e(t) + \begin{bmatrix} E & -K_f \end{bmatrix} \begin{bmatrix} \xi(t) \\ n(t) \end{bmatrix} \tag{14}$$

With stable $(A - K_f C)$, the error vector $e(t)$ will converge. If the noise vectors are absent ($\xi \equiv n \equiv 0$) , there will be a perfect estimation in steady state since $\mathrm{e(t)} \rightarrow 0$ as $\mathrm{t} \rightarrow \infty$. This fact applies to the (standard) Kalman filter, also. Inserting the $1/\beta$ at the output to scale-up the gain will leave the new filter loop stable.

3.2.2 Amplified Linear Quadratic Regulator (LTR step)

The amplified linear quadratic regulator (ALQR), is dual of the gain scaled Kalman filter (GSKF), just as the linear quadratic regulator (LQR) is dual of the Kalman filter (KF). The amplified linear quadratic regulator (ALQR) gain, K_r, are given by

$$K_r = (1/\beta)R^{-1}B^T P \tag{15}$$

with $0 < \beta < 1$. Therefore, the control signal is obtained by the amplification of the nominal controller LQR. The guaranteed multivariable margins of ALQR can be established, which correspond to the gain/phase perturbations that can be considered in all the outputs simultaneously or in an independent manner. (Prakash, 1990), (Cavalca and Kienitz, 2009). For the particular case with $Q > 0$, (Prakash, 1990) demonstrates that the ALQR loop will be stable inside certain margins, even if the system has poles in imaginary axis. Moreover, for this case, the guaranteed multivariable margins are given by:

$$GM = \beta/2, \infty \tag{16}$$

$$PM = \pm \cos^{-1}(\beta/2) \tag{17}$$

in which, GM is the guaranteed gain margin and PM is the guaranteed phase margin. For recovering with the LQR-gain, (J.C.Doyle and G.Stein, 1979) and (C.Doyle and Stein, 1981) suggest that Q should be chosen as $Q = q^2 C^T V C$, where *V* is an arbitrary symmetric and p.d. matrix, and *R* is an arbitrary p.d. matrix. This approach is the same for the procedure ALQR (Prakash, 1990). For $q \to \infty$ and if the system model is minimum phase, asymptotic recovery occurs.

4. CONTROL SPECIFICATION

Compensators designed should address the problem of stable tracking of reference trajectories(Travel and Elevation) and satisfies the following specifications: 1) reference signal tracking and disturbance rejection with error not exceeding 10% for $w \leq 0.5$ rad/s and zero steady error for the step input; 2) Attenuation of noise measurement greater than or equal to 1% with frequencies above 1000 rad/s; 3) Ensuring the robustness of stability of the controlled system.

4.1 Robust Stability

The stability robustness specification depends on a modeling error assessment. The linearized model given in Eq.(2) describes a nominal system, $G_N(s)$. In this case, a reasonable structure for the modeling error is assumed to be

$$G_R(s) = [1 + E_M(s)]\, G_N(s) \tag{18}$$

Most of modeling errors are due to high-order dynamics neglected in the modeling process, such as sensor dynamics. A first order model of the neglected dynamics is given

$$E_M(s) = \frac{1}{1 + T_{\max} s} - 1 = \frac{-T_{\max} s}{1 + T_{\max} s} \tag{19}$$

For $T_{\max} = 0.001$, the error characterization for outputs is

$$\bar{\sigma}\left[E_M(jw)\right] \leq e_M(w) = \left| \frac{-0.001s}{1 + 0.001s} \right| \tag{20}$$

Then, the stability robustness condition in closed loop is given by

$$\bar{\sigma}\left[\frac{G_N(jw)K(jw)}{I + G_N(jw)K(jw)}\right] < \frac{1 + 0.001s}{-0.001s} \tag{21}$$

4.2 Robust Performance

Requirements of the project, assign the following specifications/conditions on the actual system performance:

- Condition I: Tracking signal setpoint and rejection with error not exceeding 10% ($\alpha_d = \alpha_r = 0.1$) for frequencies to 0.5 rad/ s.

$$\text{Barriers} = \frac{\text{p(w)}}{1 - \text{E}_\text{M}(w)}, \;\; with \;\; p(w) = \alpha_r = \alpha_d, w \leq 0.5 rad/s. \tag{22}$$

- Condition II: Attenuation measurement error greater or equal to 1% with frequencies above 1000 rad/s.

$$\text{Barriers} = \frac{\alpha_\text{n}}{1 + \text{E}_\text{M}(w)}, \;\; with \;\; w \geq 1000 rad/s. \tag{23}$$

To eliminate the system error, integrators are inserted into at system output for travel angle and elevation. With insertion of integrators increases the order of system from 6 to 8. The new matrices are given by:

$$A_a = \begin{bmatrix} A & 0_{8x2} \end{bmatrix}, B_a = \begin{bmatrix} B \\ 0_{2x2} \end{bmatrix}, C_a = \begin{bmatrix} C & 0_{2x2} \\ 0_{2x6} & I_{2x2} \end{bmatrix} \tag{24}$$

Notice that the plant is not square as the number of actuators is not equal to the number of outputs as clear from the dimensions of *B* and *C*. Therefore in order to make it square, we augment the plant with a dummy input. For detailed presentations refer to (Khan, 2005).

5. DESIGN OF CONTROLLERS

The objective is to design a control system to attain robust stability and performance. Nominal stability and nominal performance are, of course, included. A TFL/LTR controllers of the PRO-version ("perturbation-reflected-to-output") will be designed to meet the stated objective. Here the TFL-gain will be a Kalman filter in the structure $\#1$ and gain-scaled Kalman filter in the structure $\#2$. The LTR-gain will be a LQR-gain and ALQR-gain, respectively.

5.1 Target Feedback Loop Design

As described in section 4.2 the robust performance barriers. The performance bounds naturally lead to bound on loop transfer at the output side. Accordingly, the low and high frequency barriers shown in Figures 4 and 5 impose requirements on the loop transfer, $G_N(jw)K(jw)$. The TFL-gains, K_f, are given by

$$K_{f_{KF}} = \begin{bmatrix} 72.3482 & 0 & -0.0845 & 0 & -0.0001 \\ 26.1749 & 0 & -0.0002 & 0 & 0.0019 \\ 0 & 7.7647 & 0 & 0.9496 & 0 \\ 0 & 30.5960 & 0 & 0.5569 & 0 \\ -0.0845 & 0 & 7.4691 & 0 & 0.9646 \\ -1.2419 & 0 & 28.3621 & 0 & 0.6993 \\ 0 & 0.9496 & 0 & 0.9987 & 0 \\ -0.0001 & 0 & 0.9646 & 0 & 0.9994 \end{bmatrix}, \; K_{f_{GSKF}} = \begin{bmatrix} 723.482 & 0 & -0.8446 & 0 & -0.0013 \\ 261.7489 & 0 & -0.0019 & 0 & 0.0193 \\ 0 & 77.6469 & 0 & 9.4958 & 0 \\ 0 & 305.9604 & 0 & 5.5687 & 0 \\ -0.8446 & 0 & 74.6905 & 0 & 9.6457 \\ -12.4188 & 0 & 283.6212 & 0 & 6.9932 \\ 0 & 9.4958 & 0 & 9.9873 & 0 \\ -0.0013 & 0 & 9.6457 & 0 & 9.9938 \end{bmatrix} \tag{25}$$

It is observed that $K_{f_{GSKF}}$-gain is $10\times$ $K_{f_{KF}}$. This happens due to the gain scaling ($\beta = 0.1$), described in section 3.2.1. Notice also that both structures satisfy the performance specifications of the real system with a bandwidth of approximately 10 rad/s.

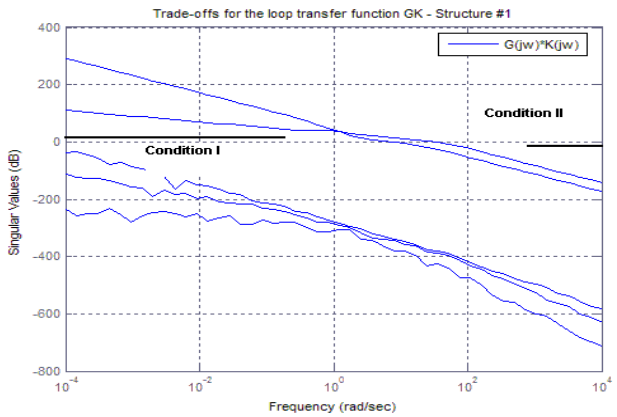

Figure 4. Performance barriers of structure # 1.

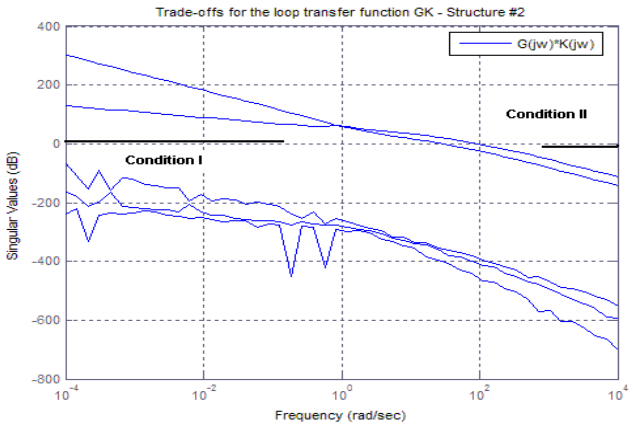

Figure 5. Performance barriers of structure # 2.

5.2 Loop Transfer Recovery

Doyle and Stein's LTR procedure will be used here. Different values were taken for the LTR-parameter q^2 and the recovery was examined graphically with both structures. For LQR (q^2=8500) and ALQR (q^2=750), the LTR-gains, K_r, respectively are

$$K_{r_{LQR}} = \begin{bmatrix} 223.2277 & 8.5485 & 227.0699 & 23.3492 & -452.4961 & -320.7462 & 206.1553 & -206.1553 \\ -223.2277 & -8.5485 & 227.0699 & 23.3492 & 452.4961 & 320.7462 & 206.1553 & 206.1553 \end{bmatrix} \quad (26)$$

$$K_{r_{ALQR}} = \begin{bmatrix} 707 & 47.6 & 719.8 & 131.5 & -1364.8 & -984.2 & 612.4 & -612.4 \\ -707 & -47.6 & 719.8 & 131.5 & 1364.8 & 984.2 & 612.4 & 612.4 \end{bmatrix} \quad (27)$$

Figures 6 and 7 illustrate the best recovery obtained for two different structures. For comparison of the controllers, considered $R = 0.1I_2$ (I_2 is a 2×2 identity matrix), sufficiently close of TFL (Target Feedback Loop).

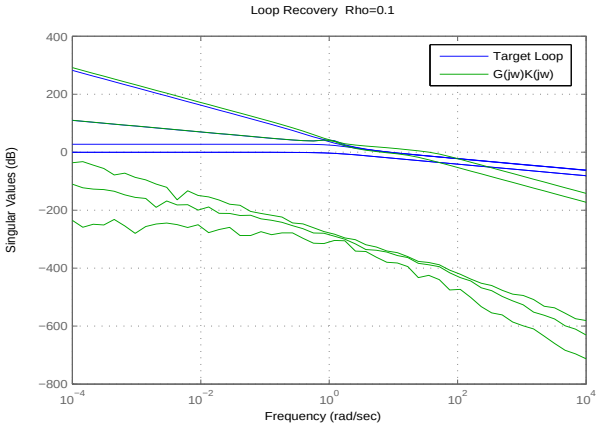

Figure 6. LTR of structure # 1.

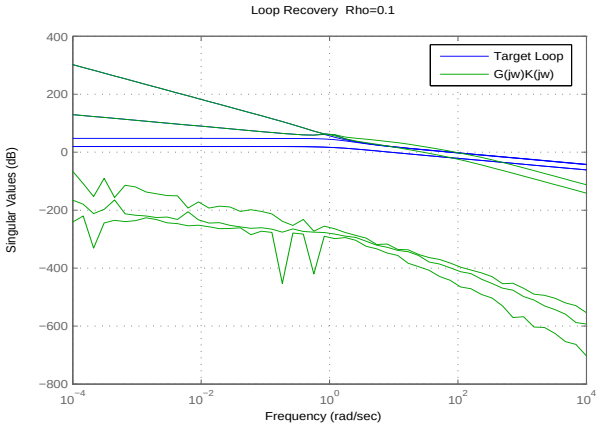

Figure 7. LTR of structure # 2.

It is observed that the recovery using ALQR-gain with $\beta = 0.1$ was better than using LQR-gain. Note also that there was an increase in stability margin given by,

$$PM_{ALQR} = \pm \cos^{-1}(\beta/2) = \pm 87.1^{\circ} \quad (28)$$

6. RESULTS AND DISCUSSION

6.1 Robust Stability

Before we can assert that the design process is complete, we must verify robust stability. In the loop shaping process, we ensured that the bandwidth of the loop transfer was less than that of uncertain function, $e_M(w)$. A verification of Eq. (21) will guarantee robust stability for both structures. Figures 8 and 9 verifies the above condition graphically.

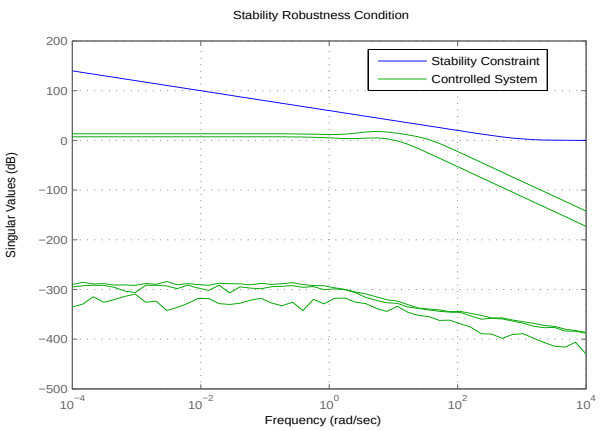

Figure 8. Robust stability of structure # 1.

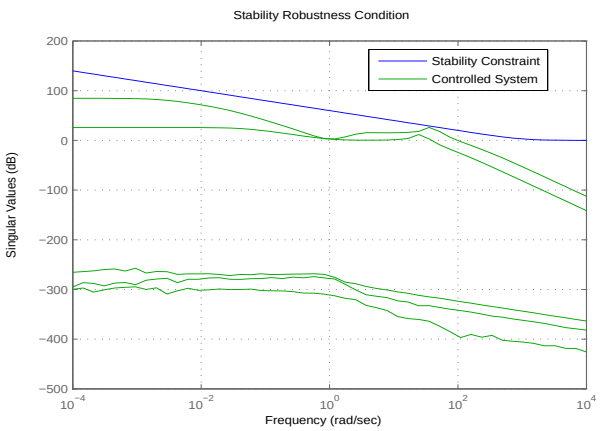

Figure 9. Robust stability of structure # 2.

One concludes that the closed loop system will be stable for errors and perturbations represented by the uncertainty model.

6.2 Closed Loop Response

In two experiments using the two structures of controllers, elevation and travel reach the desired reference system without steady errors not exceeding 10%. These responses obtained in the experiment where the elevation and the travel was kept constant at 20° and 180°, respectively. As can be verified below,

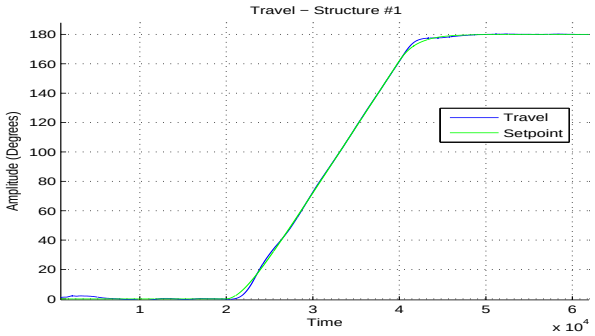

Figure 10. Travel of structure # 1.

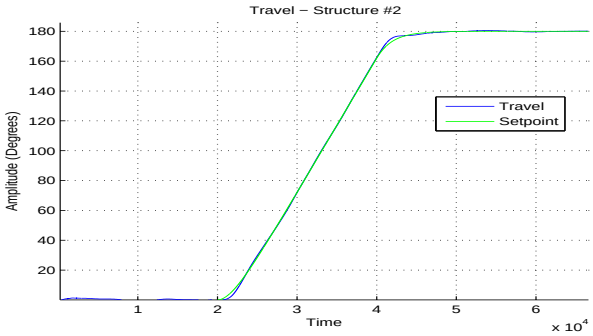

Figure 11. Travel of structure # 2.

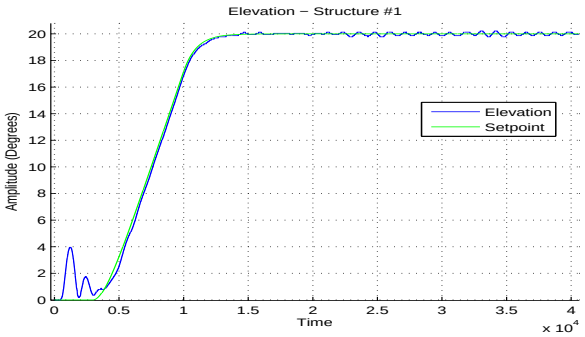

Figure 12. Elevation of structure # 1.

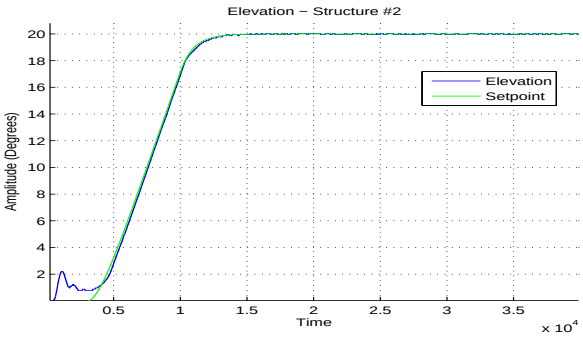

Figure 13. Elevation of structure # 2.

However, the helicopter presents variations of the dynamics of the axis of pitch around 5° in both structures, while the linear model variations are around 0°, as can be verified in Figures 14 and 15. These differences may be caused by some aerodynamic effect in the system that was neglected in the modeling.

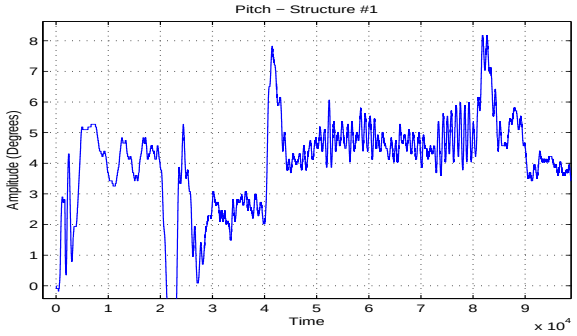

Figure 14. Pitch of structure # 1.

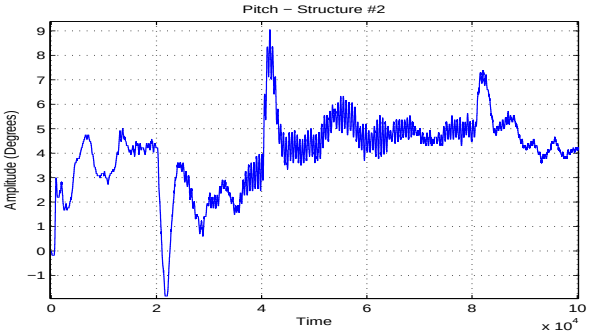

Figure 15. Pitch of structure # 2.

The comparative study, experiments performed by using the nonlinear model of the helicopter, showed that the robust controller TFL/LTR using the structure $\#2$ is superior to standard LQG/LTR, mainly mainly during transient regime providing better tracking of the trajectories of stable reference.

7. CONCLUDING REMARKS

When we compare the transient amplitude and the settling time in structures #1 and #2, we observe that structure #2 design produces a compensator with better performance than LQG/LTR design. The new structure also guarantees a smaller and a better LTR-gain for recovery to a higher phase margin. On the other hand, the gains TFL and LTR were higher than the standard structure (LQG/LTR), favoring the saturation of the actuators. Finally, both structures show qualities and difficulties to design a controller that satisfy all robustness and performance requirements.

8. ACKNOWLEDGEMENTS

The authors acknowledge all support provide by CNPq

9. REFERENCES

Athans, M., 1986. "A tutorial on the LQG/LTR method". *American Control Conference*, pp. 1–7.

Cavalca, M.S.M. and Kienitz, K.H., 2009. "Application of TFL/LTR robust control techiniques to failure accommodation". *20th International Congress of Mechanical Engineering*, pp. 1–8.

C.Doyle, J. and Stein, G., 1981. "Multivariable feedback design: Concepts for a classical/modern synthesis". *IEEE Transactions on Automatic Control*, Vol. AC-26, pp. 4–16.

da Cruz, J.J., 1996. *Controle Robusto Multivariável*. Universidade de São Paulo- EDUSP.

J.C.Doyle and G.Stein, 1979. "Robustness with observers". *IEEE Transactions on Automatic Control*, Vol. AC-24, pp. 607–611.

Khan, A.Q., 2005. "LQG/LTR based controller design for three degree of freedom helicopter/twin rotor control system".

Lopes, R.V., 2007. *Modelagem e controle preditivo de um helicóptero com três graus de liberdade*. Master's thesis, Instituto Tecnológico de Aeronáutica.

Maia, M.H., 2008. *Controle preditivo robusto de um helicóptero com três graus de liberdade sujeito a perturbações externas*. Master's thesis, Instituto Tecnológico de Aeronáutica.

Prakash, R., 1990. "Target feedback loop/loop transfer recovery (TFL/LTR) robust control design procedures". *29 th Conference on Decision and Control*, pp. 1203–1209.

Rubens, K.H.K.e.R.K.H.G., 2009. "Projeto de um controlador robusto para um modelo de um helicóptero com três graus de liberdade baseado no método LQG/LTR". *3 ž CTA-DLR Workshop on Data Analysis & Flight Control*.

Skogestad, S. and Postlethwaite, I., 2001. *Multivariable Feedback Control: Analysis and design*. John Wiley & Sons.

10. Responsibility notice

The author(s) is (are) the only responsible for the printed material included in this paper